Jestr

Journal of Engineering Science and Technology Review 15 (3) (2022) 99 - 108

JOURNAL OF
Engineering Science and Technology Review

Research Article

www.jestr.org

Characteristics of a Two-component Waterborne Acrylic Emulsion Waterproof Coating based on Underground Engineering

Dong Yan[1,2], Songbai Chen[1], Xuedang Xiao[2,*], Fengxiang Zhang[1] and Inchen Chen[3]

[1] *College of Architecture and Civil Engineering, Xinyang Normal University, Xinyang 464000, China*
[2] *Xinyang Lingshi Technology Co., Ltd., Xinyang 464000, China*
[3] *International College, Krirk University, Bangkok 10220, Thailand*

Received 22 April 2022; Accepted 8 July 2022

Abstract

Acrylic waterproof coatings have good performance, but their application is limited by their high cost. In addition, few studies explored the waterproofing and impermeability characteristics of these coatings. Based on experimental and theoretical analyses, this study prepared a waterproof coating composed of acrylate polymer emulsion (pure acrylic emulsion) and low-cost styrene–acrylate copolymer emulsion (styrene–acrylic emulsion) to improve the performance, reveal the impermeability mechanism, and decrease the cost. Orthogonal and single-factor tests were carried out to analyze the mechanical, waterproofing, and impermeability properties of the coating. The optimal proportion of the waterproof coating was determined. Results show that combining styrene–acrylic emulsion and pure acrylic emulsion can enhance the performance and reduce the cost of waterproof coatings. In addition, performance improvement is positively correlated with the mesh number of heavy calcium carbonate, and the water pressure of an 800-mesh heavy calcium carbonate coating is increased to 1.4 MPa. In the anti-permeability test, the surface of the coating film bulges under the action of water pressure, and the bulges rupture and water seep occurs under continuous pressure. When the dosage of tributyl phosphate is 0.35%, the water pressures under the coating bulges and water seep are 0.7 and 1.5 MPa, respectively. This study can serve as a basis for the study and impermeability evaluation of acrylic emulsion waterproof coatings.

Keywords: Acrylic waterproof coatings, Two-component, Underground engineering, Impermeability

1. Introduction

Acrylic emulsion waterproof coatings have several advantages [1], such as good film-forming performance, high elongation at break, non-toxicity, tastelessness, no solvent pollution, waterproof, heat insulation, cold construction, and convenient maintenance. These coatings are widely used in tunnel engineering, underground garages, and interior walls. Demands for the application of acrylic waterproof coatings have increased, and the related technical studies have achieved great progress. In fact, an increasing number of studies focused on the design, production, and application of acrylic waterproof coatings [2]. The principal component of most acrylate emulsion waterproof coatings is acrylate polymer emulsion (pure acrylic emulsion) or modified acrylic emulsion. Jasperson [3] developed elastic and durable waterproof coatings with acrylic and vinyl polymer emulsions as the main film-forming materials, which can be used for the waterproofing of roofs and exterior walls, thus achieving high elasticity and good durability.

However, with their long-term development, acrylic emulsion waterproof coatings have become increasingly multifunctional, and their waterproofing and impermeability effects have been enhanced. The performance of acrylic waterproof coatings is improved at the expense of high production cost. In the design process, pure acrylic emulsion or modified styrene–acrylate copolymer emulsion (styrene–acrylic emulsion) is used as the main liquid component. In addition to the high difficulty in technology and poor economy, the waterproofing, impermeability, physical, and mechanical properties of acrylic waterproof coatings are influenced by many factors, which complicate the study of acrylic waterproof coatings.

Numerous studies aimed to improve the waterproofing, impermeability, physical, and mechanical properties and decrease the production costs of acrylic emulsion waterproof coatings [4-6]. However, studies on the impermeability of coatings in underground engineering remain to have problems, such as the deviation from the actual working state and good performance but high cost in practical engineering applications. Therefore, how to accurately predict the impermeability of the waterproof coating, decrease the application cost, and determine the coupling relationship between the waterproof coating and mortar base in the actual working state of waterproof coatings in underground engineering is an urgent problem to be solved.

Based on the above analyses, the present study combined low-cost non-modified styrene–acrylic emulsion with pure acrylic emulsion to establish an experimental model of waterproof coating on the mortar base block. The waterproofing, impermeability, physical, and mechanical properties of the new waterproof coating were analyzed. This study is expected to reveal the impermeability of the waterproof coating, decrease the production cost, and improve the performance of acrylic coatings, thereby

*E-mail address: lingshixxd@163.com
ISSN: 1791-2377 © 2022 School of Science, IHU. All rights reserved.
doi:10.25103/jestr.153.10

providing a reference for the development and optimization of waterborne acrylic emulsion waterproof coatings.

2. State of the art

At present, numerous scholars have analyzed organic polymer waterproof coatings. Bożena et al. [7] studied the WAXD diffraction patterns and SEM imaging patterns of polyurethane coating films modified by hydrotalcite nanoparticles, but a detailed analysis of their physical and mechanical properties remains lacking. Pilch-Pitera et al.[8] prepared a transparent coating with polyurethane, hydrotalcite, and aminododecanoate and studied its elasticity and surface free energy, but the waterproofing performance of this coating was not evaluated. Hussein et al.[9-10] improved the hydrophobicity and mechanical properties of polymer waterproof coatings by mixing graphene and carbon fibers into waterproof coatings, providing a reference for studying the impact resistance of coatings. Jin et al.[11] developed a polyurethane breathable waterproof coating film modified by polyethylene glycol macromolecules, providing a reference for studying the breathability of waterproof coatings. Ye and Zhou [12] determined the influence of inorganic fillers on the performance of one-component acrylate waterproof coatings.

Wu et al.[13-14] modified a polymer waterproof coating with nano-SiO_2 particles and studied its self-cleaning ability. Jia [15] prepared two waterproof coatings composed of polyethylene–vinyl acetate emulsion and styrene–acrylic emulsion and evaluated their dry film water absorption, physical and mechanical properties, and water resistance. Peruchi et al.[16] prepared hydrotalcite particle- and anionic-modified polyurethane coatings and evaluated their contact angle, hardness, hydrophobicity, and scratch resistance. Guo et al.[17] modified a butyl acrylate coating with an intumescent combustion improver and deduced the flame retardant mechanism of the hydrophobic fireproof coating. Xiao et al[18-19] used styrene–acrylic emulsion, white cement, and rutile as base materials to design waterproof coatings with high solar reflectivity. Zhang [20] discussed the influence of the mesh number of quartz powder on the tensile properties of waterproof coatings. Hu et al.[21] modified waterproof coatings based on the hydrophobicity of loess, which provided a basis for reducing the water absorption rate of waterproof coatings. Considering the characteristics of polyurethane, Zong et al.[22] modified two-component polyurethane with epoxy resin, which provided a reference for the self-repair of waterproof coatings.

The above results focused on the multi-functional modification and physical and mechanical properties of waterproof coatings but did not consider their waterproofing characteristics, especially the impermeability of special coatings in underground engineering. Accordingly, the present study applied a waterproof coating to a prefabricated mortar base block and established an impermeability test model of the waterproof coating. On the basis of the characteristics of the waterproof coating in underground engineering, the impermeability, tensile strength, and elongation at break of the two-component waterproof coating were discussed, and the coupling relationship of impermeability between the waterproof coating and the mortar base was deduced, which provides a basis for the optimization and test of waterproof coatings.

The remainder of this study is organized as follows. In Section 3, the physical and mechanical properties and water impermeability were examined in a three-factor four-level orthogonal test, and the initial proportion of the waterproof coating was determined. In Section 4, the influence of the mesh number of heavy calcium carbonate and the content of tributyl phosphate on the waterproofing, impermeability, physical, and mechanical properties of the waterproof coating were studied. The optimal mesh number of heavy calcium carbonate and the content of tributyl phosphate were determined. Finally, Section 5 summarizes this study and draws relevant conclusions.

3. Methodology

3.1 Test scheme

Orthogonal test scheme. The initial ratio was determined by performing a three-factor four-level orthogonal test (Table 1, Orthogonal Test Scheme Table). The ratio of styrene–acrylic emulsion to pure acrylic emulsion and the proportions of film-forming additives and sodium hexametaphosphate aqueous solution (40% by mass) in liquid components were taken as the three factors in the orthogonal test. Then, the water impermeability, tensile strength, and elongation at break at each ratio were investigated. The proportions of wetting agent, silane coupling agent, and tributyl phosphate in liquid components were 0.2%, 0.3%, and 0.7%, respectively. The solid components were 325-mesh heavy calcium and 1250-mesh talcum powder with a mass ratio of 9: 1. At this stage, the mass ratio of liquid-to-solid components (hereinafter referred to as liquid powder ratio) was 1: 1.

Table 1. Orthogonal test scheme table

Serial number	1	2	3	4	5	6	7	8	9	10	11	12	13	14	15	16
A Proportion of pure acrylic emulsion and styrene acrylic emulsion	0.5	0.5	0.5	0.5	0.37	0.37	0.37	0.37	0.23	0.23	0.23	0.23	0.10	0.10	0.10	0.10
B Proportion of alcohol ester 12 in liquid components (%)	0.50	1.50	2.50	3.50	0.50	1.50	2.50	3.50	0.50	1.50	2.50	3.50	0.50	1.50	2.50	3.50
C Proportion of 40% sodium hexametaphosphate aqueous solution to liquid component (%)	0.75	1.75	2.75	3.75	1.75	0.75	3.75	2.75	2.75	3.75	0.75	1.75	3.75	2.75	1.75	0.75

Test scheme of inorganic filler modification. The 7th and 8th groups with better performance in the orthogonal test were selected to investigate the effects of 200-mesh, 325-mesh, 600-mesh, and 800-mesh heavy calcium on the physical, mechanical, waterproofing, and impermeability properties of the coating. The optimal mesh number of heavy calcium was determined. When 600-mesh and 800-mesh heavy calcium carbonate was used, the coating film cracked after drying. At this stage, the 40% sodium hexametaphosphate aqueous solution was replaced with 5% sodium hexametaphosphate solution by carrying out a coating test, and the liquid–powder ratio was adjusted to 1: 0.93. Other components remained unchanged.

Test scheme of defoamer modification. For the seventh formula determined by inorganic filler modification, tributyl phosphate accounting for 0%, 0.35%, 0.7%, 1.05%, and 1.4% of the liquid components was employed to study the influence on the physical, mechanical, waterproofing, and impermeability properties of the coating.

3.2 Materials and instruments

In the study, styrene–acrylate copolymer emulsion, acrylate copolymer emulsion, alcohol ester 12, sodium hexametaphosphate, wetting agent, silane coupling agent, tributyl phosphate, and deionized water were used as liquid components. Solid components included 200-mesh, 325-mesh, 600-mesh, and 800-mesh heavy calcium and 1250-mesh talcum powder.

The main test instruments included a smearing film frame, a punching machine, a dumbbell cutter, a thickness gauge, a stirrer, a tensile tester, an impermeability tester (used for waterproof coating), and an impermeability tester (used for mortar).

3.3 Particle update rules

The tensile strength and elongation at break were studied in accordance with Chinese Architecture Industry Standard JC/T 864-2008 (polymer emulsion architectural waterproof coating). Under the standard condition (23℃, relative humidity 50%), the heavy calcium and talcum powder were mixed evenly at the mass ratio of 9: 1 for later use. The mixed styrene–acrylic emulsion and pure acrylic emulsion were stirred at 400 rad/min for 1 min. The wetting agent and sodium hexametaphosphate solution were dispersed at 600 rad/min for 3 min. Alcohol ester 12 was added and dispersed at 400 rad/min for 1 min. Silane coupling agent was added and dispersed at 400 rad/min for 1 min. The solid and liquid components were mixed and dispersed for 3 min at 800 rad/min. Finally, tributyl phosphate was added and dispersed at 200 rad/min for 1 min. The adjusted samples were coated on the film frame at 24 h intervals, and the final film thickness was 1.5 mm. The specimen cured for 168 h was cut into a dumbbell shape with a cutter and a punching machine (Fig. 1), and the thickness was measured with a thickness gauge. Parallel markings were drawn with a spacing of 35 mm on the specimen, and the width of the specimen was 6mm. The specimen was fixed on the tensile testing machine (Fig. 2), and the maximum tensile force and

the distance between the lines when breaking were recorded. The tensile strength was calculated as follows:

$$T = \frac{P}{6 \times D} \tag{1}$$

where T is the tensile strength in MPa, P is the maximum tensile force in n, and D is the thickness of the specimen in mm. The elongation at break of the specimen was calculated as follows:

$$E = \frac{L - 35}{35} \times 100\% \tag{2}$$

where E is the elongation at break, and L is the marking distance at break in mm. The arithmetic mean of tensile strength and elongation at break of five specimens are taken as the test result.

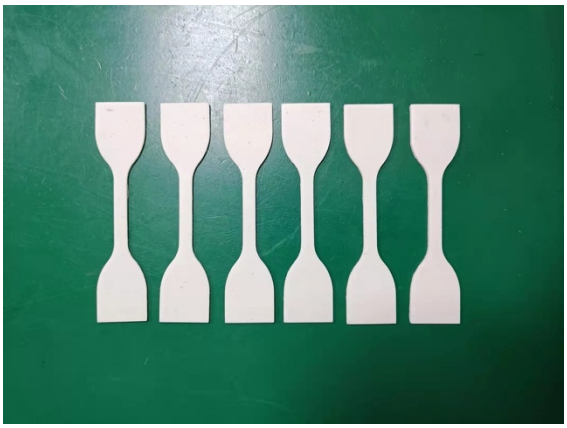

Fig. 1. Dumbbell specimen

Fig. 2. Tensile testing machine

3.4 Test method for impermeability

An impermeability test was carried out in accordance with the Chinese architecture waterproofing coating test method (GB/T 16777-2008). The film cured to the specified age in Section 3.3 was cut into three specimens with the size of 150 mm × 150 mm × 1.5 mm, and the air in the impermeability tester (Fig. 3) was exhausted. The specimens were placed on the permeable disk of the tester. As shown in Fig. 4, the specimen was covered with a metal mesh and a seven-hole disc, and the specimen was clamped and slowly pressurized. The water pressure was retained at 0.3 MPa for 30 min, and whether the non-upcoming water surface was permeable was

observed. The specimen was judged to be qualified when no water seepage was observed.

Fig. 3. Impermeability tester

Fig. 4. Diagram of specimen installation

3.5 Test method for permeability

Ordinary cement mortar specimens were prepared according to the mass ratio of water, cement, and sand of 1: 1.46: 4.37 and the consistency of 47 mm. The specimens prepared in Section 3.3 were coated on the downstream face of the mortar specimens twice at the interval of 24 h, and the coating thickness was 2.5 mm. Three specimens were prepared in each group (Fig. 5). The specimens were cured for 6 days under standard conditions. Six specimens without coating were cured under the same conditions. The test was carried out at room temperature, and the cured uncoated specimens were sealed with sealing materials. The air in the impermeability tester (Fig. 6) was exhausted, and the specimens were placed in the tester (Fig. 7). The tester was started, and the pressure was increased by 0.1 MPa every 1 h until water seepage. The water pressure of the fourth specimen in the six specimens was 0.4 MPa. The sealing and pressure modes of the coating specimen were the same as those mentioned above. The water pressure of the second specimen film bulging (hereinafter referred to as the bulging water pressure) and the water pressure of water seepage (hereinafter referred to as the water seepage pressure) were recorded as the test data.

Fig. 5. Impermeability specimen

Fig. 6. Impermeability tester

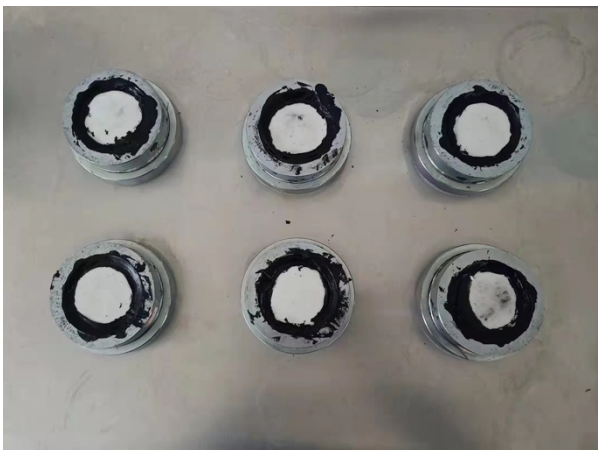

Fig. 7. Impermeability specimen installation

4 Result Analysis and Discussion

4.1 Analysis of orthogonal test results

Based on the test scheme in Section 3.1, the orthogonal test results (Tables 2, 3 and 4) were obtained.

Table 2. Orthogonal test results of tensile strength and elongation at break

Serial number	1	2	3	4	5	6	7	8	9	10	11	12	13	14	15	16
Tensile strength (MPa)	1.32	1.08	1.05	0.84	1.37	1.57	1.05	1.00	1.82	1.64	1.17	0.90	1.90	1.52	1.17	0.95
Elongation at break (%)	149	158	164	193	168	180	231	280	176	196	218	237	186	237	186	233

Table. 3. Orthogonal test results of impermeability

Serial number	1	2	3	4	5	6	7	8
Impermeability	Qualified	Qualified	Unqualified	Unqualified	Qualified	Qualified	Qualified	Qualified

Table. 4. Orthogonal test results of impermeability

Serial number	9	10	11	12	13	14	15	16
Impermeability	Unqualified	Unqualified	Unqualified	Unqualified	Unqualified	Unqualified	Unqualified	Unqualified

The range of the orthogonal test results was analyzed (Tables 5 and 6). The primary and secondary orders of factors influencing the tensile strength and elongation at break of the waterproof coating were B (alcohol ester 12% of liquid component) > A (pure acrylic emulsion and styrene–acrylic emulsion ratio) > C (40% sodium hexametaphosphate solution accounts for liquid component ratio).

As shown in Tables 5 and 6, the film-forming additives significantly influenced the mechanical properties of the waterproof coating. The film-forming additives increased the plasticity of the coating film, which improved the mobility of the polymer molecular chains and decreased the glass transition temperature of the acrylic emulsion. The emulsion transformed from glassy state to highly elastic state, which improved the flexibility of the waterproof coating after drying. When the content of alcohol ester 12 increased, the flexibility of the waterproof coating enhanced correspondingly, which decreased the tensile strength and increased the elongation at break.

Table 5. Analysis table of tensile strength range

K_1	4.29	6.41	5.01
K_2	4.99	5.81	4.52
K_3	5.53	4.44	5.39
K_4	5.54	3.69	5.43
$\overline{K_1}$	1.43	1.60	1.25
$\overline{K_2}$	1.66	1.45	1.13
$\overline{K_3}$	1.84	1.11	1.35
$\overline{K_4}$	1.85	1.23	1.36
Range R	**0.42**	**0.49**	**0.23**
Order	**B>A>C**		

Table 6. Analysis table of elongation at break range

K_1	6.64	6.79	7.80
K_2	8.59	7.71	7.49
K_3	8.27	7.99	8.57
K_4	8.42	9.43	8.06
$\overline{K_1}$	1.66	1.70	1.95
$\overline{K_2}$	2.15	1.93	1.87
$\overline{K_3}$	2.07	2.00	2.14
$\overline{K_4}$	2.11	2.36	2.02
Range R	**0.49**	**0.66**	**0.27**
Order	**B>A>C**		

As shown in Tables 5 and 6, the ratio of pure acrylic emulsion to styrene–acrylic emulsion obviously influenced the mechanical properties of the coating, which is second only to alcohol ester 12. The study results showed that the film composed of pure acrylic emulsion is much more flexible than that composed of pure acrylic emulsion [23]. When the ratio of pure acrylic emulsion to styrene–acrylic emulsion was increased, the tensile strength decreased while the elongation at break increased. As shown in Tables 3 and 4, when the ratio of pure acrylic emulsion to styrene–acrylic emulsion was too low, the water impermeability test failed because of the benzene rings in the polymer molecules of styrene–acrylic emulsion. Analysis of steric effects showed that the molecular gap of styrene–acrylic emulsion was larger than that of pure acrylic emulsion, and the gap caused by the stacking of particles during the water volatilization of styrene–acrylic emulsion was larger than that of pure acrylic emulsion. Under the action of water pressure, the coating with more styrene–acrylic emulsion was more likely to swell and become damaged because of water penetration. When a suitable amount of pure acrylic emulsion was added, the particles of pure acrylic emulsion can be stacked among the particles of styrene–acrylic emulsion in the drying process of waterproof coating. Therefore, it has good waterproof effect. However, excessive addition of pure acrylic emulsion and film-forming additives increased the plasticity of the coating film, which caused water penetration at the needle holes.

As shown in Tables 5 and 6, the influence of sodium hexametaphosphate aqueous solution on the tensile strength and elongation at break of the waterproof coating was less obvious than that of film-forming additives and pure acrylic emulsion styrene–acrylic emulsion. Sodium hexametaphosphate is used as dispersant. One end of its active group can be adsorbed on the surface of inorganic filler particles, and the other end can be adsorbed on emulsion particles to form an adsorption layer. These phenomena generate charge repulsion, disperse and suspend inorganic filler to avoid flocculation, and reduce the internal defects of the coating after drying. However, sodium hexametaphosphate, as a surfactant, can adsorb and anchor the bubbles in the emulsion phase by adsorbing at the gas–liquid interface, resulting in micro-voids in the waterproof coating after drying. The coating film was not dense enough and easy to break after drying. Therefore, it exerted less obvious influence on the tensile strength and elongation at break of the coating film.

With the comprehensive properties of the waterproof coating materials, groups 7 and 8 in the orthogonal test exhibited excellent physical and mechanical properties and waterproofing performance.

4.2 Effect of different meshes of heavy calcium carbonate on the properties of waterproof coating materials

Groups 7 and 8 with better physical, mechanical, and water impermeability properties than the other groups in the

orthogonal test were selected, and the effects of 200-mesh, 325-mesh, 600-mesh, and 800-mesh heavy calcium on the tensile strength, elongation at break, and water impermeability were analyzed.

When 800-mesh and 600-mesh heavy calcium carbonate was used, the coating film cracked after drying (Fig. 8). The cracks only appeared on the front side of the coating film, whereas the back side of the coating film was smooth and had no cracks (Fig. 9). Film cracking can be ascribed to several reasons. (1) The test temperature cannot reach the lowest film-forming temperature of acrylic emulsion. (2) The tension on the surface of the prepared material was too large; the edge of the coating dried faster, but the middle part dried slower, which resulted in cracks. (3) Given the excessive amount of inorganic fillers or the large specific surface area, the amount of emulsion wrapped around the filler particles was insufficient, which caused the coating film to crack after drying. (4) The material prepared had excessive bubbles because of surfactant or excessive mechanical stirring. During the drying of the coating film, the emulsion particles in the middle of adjacent bubbles were close to each other, agglutinated, and were finally destroyed. Bubbles were connected, and cracks were generated. (5) Two pieces of coating film cannot be connected and cracked because of excessive use of mold release agent.

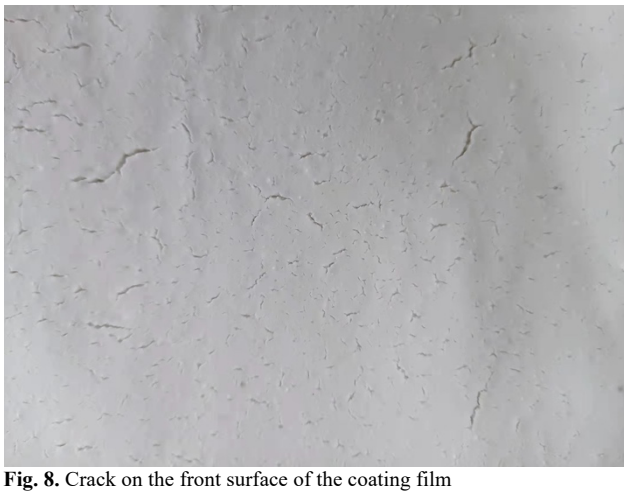

Fig. 8. Crack on the front surface of the coating film

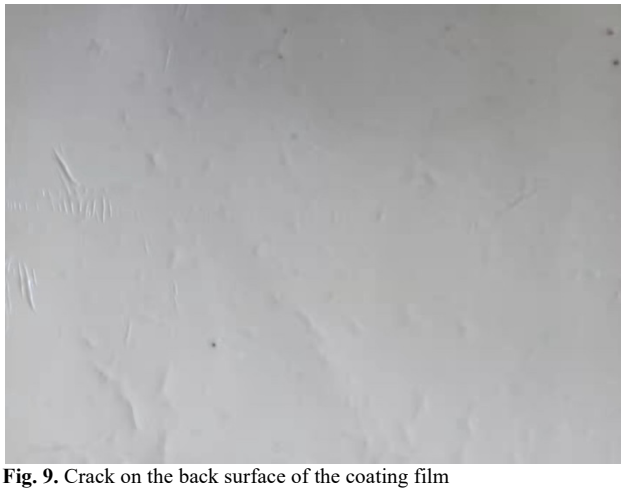

Fig. 9. Crack on the back surface of the coating film

Reason (1) was eliminated by carrying out the test in the standard state, and the cracks in the coating film did not penetrate through the cross section of the coating film. The back surface was smooth and uniform, and reasons (2), (3), and (5) could be eliminated. Cracks only existed on the surface, which is in line with the characteristics of bubbles floating in liquid. The coating film cracked because of excessive bubbles. The surfactant in the formula was mainly composed of sodium hexametaphosphate solution and wetting agent. After removing the respective coatings of the two substances, the sodium hexametaphosphate solution caused excessive bubbles.

Considering the above problems, the sodium hexametaphosphate solution with different mass fractions was employed to test the coating film, and whether the coating film cracked was observed. On the basis of the analysis in Section 4.1, we concluded that the sodium hexametaphosphate solution exerted minimal influence on the waterproof coating, and the performance of the coating film with different mass fractions of sodium hexametaphosphate solution was not investigated. Finally, 40% sodium hexametaphosphate solution was changed to 5% sodium hexametaphosphate solution, and the liquid–powder ratio was changed to 1: 0.93 to decrease the consistency.

By using 200-mesh, 325-mesh, 600-mesh, and 800-mesh heavy calcium, the tensile strength, elongation at break, and water impermeability of groups 7 and 8 after changing the ratio were investigated.

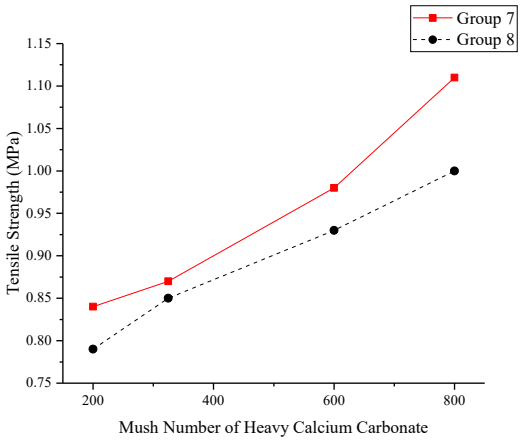

Fig. 10. Test results of tensile strength

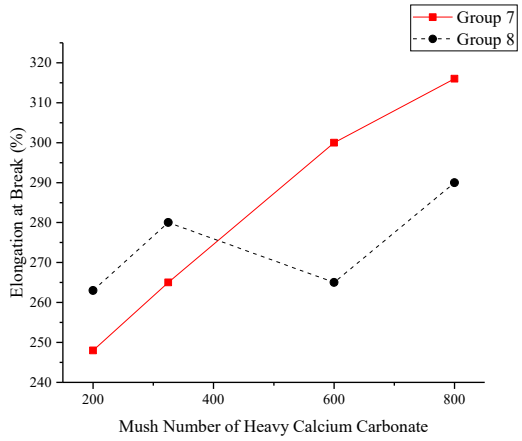

Fig. 11. Test results of elongation at break

Through the test, the characteristic diagrams of the tensile strength and elongation at break of the two groups with the mesh number of heavy calcium were obtained. As shown in Figs. 10 and 11, the tensile strength and elongation at break

of groups 7 and 8 generally increased with increasing mesh number of heavy calcium. When the mesh number of the filler was low, the particle size of heavy calcium particles was relatively large, which cannot be fully wrapped after mixing with liquid phase materials. After the water was dried, the emulsion particles contacted and agglomerated to form a loose network structure, which led to low tensile strength and elongation at break. When the mesh number of heavy calcium carbonate was high, the dispersed heavy calcium carbonate particles were uniformly dispersed in the liquid phase material and a dense coating film was formed, which reduced the internal microscopic defects of the polymer film and improved the tensile strength and elongation at break.

Table 7 shows the impermeability test results of groups 7 and 8. Group 7 was qualified, whereas group 8 was only qualified when 800-mesh heavy calcium carbonate was used as an inorganic filler. Fig. 12 presents the water penetration on the back surface of group 8. The sealing ring diffused to the surroundings, and trace of the round sealing ring squeezing the specimen on the water surface of the specimen was observed (Fig. 13). Considering that the dosage of film-forming additives in the eighth composition can improve the flexibility of acrylic emulsion coating, we can conclude that the water permeability in group 8 was caused by excessive flexibility. As a result, the specimen was squeezed and thinned by the sealing ring, and the coating swelled at this position under the action of 0.3 MPa water pressures, which declined the waterproof effect. However, 800-mesh heavy calcium coating was used in group 8, and the compactness and physical and mechanical properties of this group were higher than those of the other groups. Therefore, no water penetration occurred.

Table 7. Test results of water impermeability

Mesh number of calcium carbonate	200-mesh heavy calcium	325-mesh heavy calcium	600-mesh heavy calcium	800-mesh heavy calcium
Group 7	Qualified	Qualified	Qualified	Qualified
Group 8	Unqualified	Unqualified	Unqualified	Qualified

Fig. 12. Water permeability side

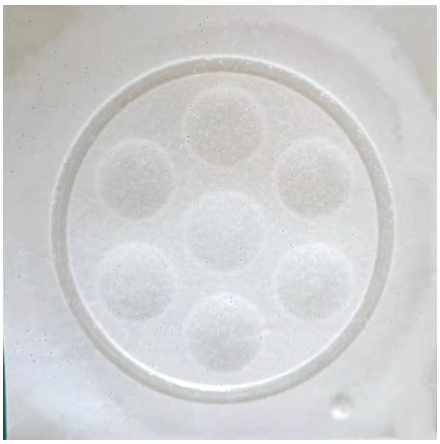

Fig. 13. Side subjected to water pressure

The impermeability of group 7 was investigated by performing the impermeability test. Under the action of water pressure, the surface of waterproof coating bulged (Fig. 14), and the continuous pressure swelled and the coating broke and leaked water (Fig. 15). In Fig. 16, with the increase in the mesh number of heavy calcium carbonate, the bulging and seepage water pressures of the waterproof coating generally increased. When 800-mesh heavy calcium carbonate was used, the impermeability effect increased sharply, and the bulging and seepage water pressures were 1.3 and 1.4 MPa, respectively. Given the small particle size of the used heavy calcium carbonate, the immersion depth of the coating in the mortar increased before the water evaporated, and the waterproof coating crosslinked into a film within a certain depth of the mortar, which reduced the inter-connected internal gap of the mortar surface system and improved the caulking and plugging effect of the waterproof coating on the mortar base.

Fig. 14. Coating bulging

Fig. 15. Coating bulging rupture and water seepage

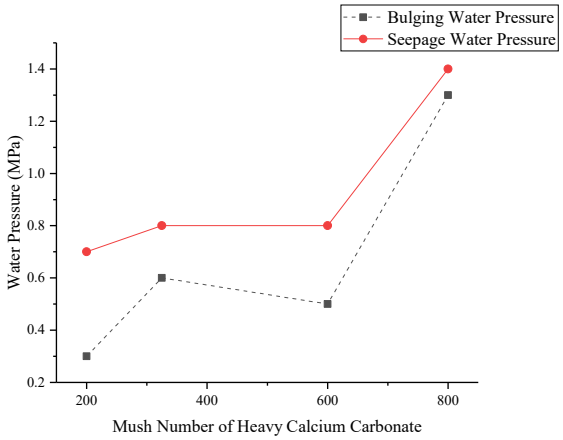

Fig. 16. Test results of permeability test

4.3 Effect of tributyl phosphate on property of waterproof coating material

The bubbles in the coating film obviously decreased with increasing amount of tributyl phosphate. Samples with different tributyl phosphate contents were cut into small parts with the size of 10 mm × 10 mm × 1.5 mm, and the cross section was cut with a knife. As shown in Fig. 17, with the increase in defoamer ratio, the air bubbles of the waterproof coating obviously decreased after drying. No obvious air bubbles were observed in the cross section of the coating film when defoamer accounted for 1.05% and 1.4% of the liquid components. This result can be ascribed to the fact that tributyl phosphate can quickly diffuse at the interface of the foam, reduce its surface tension, and make the foam thin and finally burst. As shown in Table 8, the coating had a porous internal structure when the defoaming agent was not added. Under the action of water pressure, a water seepage channel was generated, which caused the water penetration of the specimen.

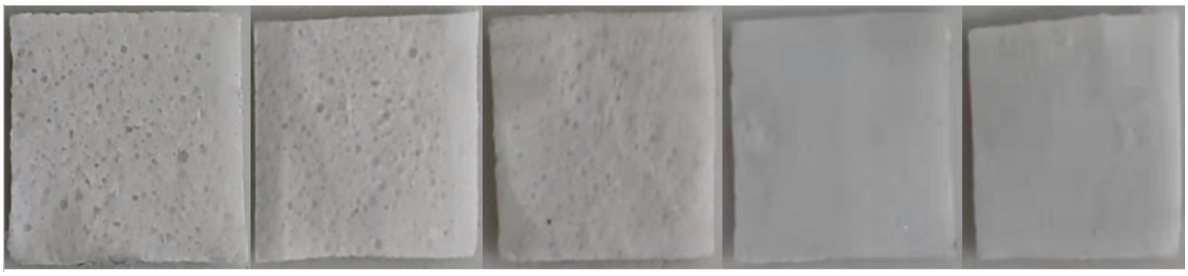

Fig. 17. Cross-section of specimen

Table. 8. Impermeability test results

Mass ratio of defoamer (%)	**0**	**0.35**	**0.7**	**1.05**	**1.4**
Test results	Unqualified	Qualified	Qualified	Qualified	Qualified

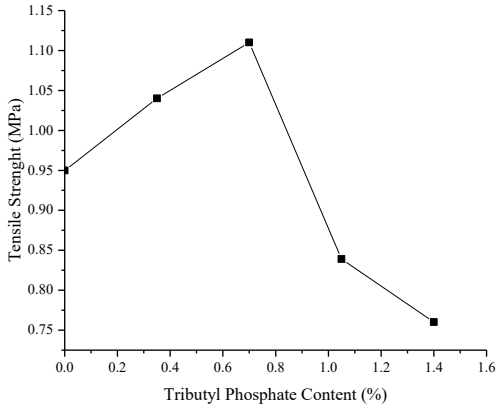

Fig. 18. Tensile strength results

As shown in Fig. 18, the tensile strength of the coating film initially increased and then decreased with the increase in defoamer content. When the content of tributyl phosphate was less than 0.7%, the tensile strength of the coating film was mainly determined by the defoaming effect of tributyl phosphate, and the internal microscopic cavities of the coating film were reduced, which improved the compactness and tensile strength of the coating film. When the content of tributyl phosphate was more than 0.7%, the tensile strength of the coating film was determined by the plasticity of tributyl phosphate. Small tributyl phosphate molecules can enter the polymer molecular structure, thus reducing the rigidity of the coating after drying, and the tensile strength decreased. In Fig. 19, the elongation at break of the waterproof coating was obvious with the increase in defoamer dosage, up to 351%. After the compactness of the waterproof coating improved with the increase in defoamer dosage, the specimen gradually changed from dense state to honeycomb until fracture in uniform tension. The elongation at break of the coating specimen improved when the internal defects of the coating were reduced.

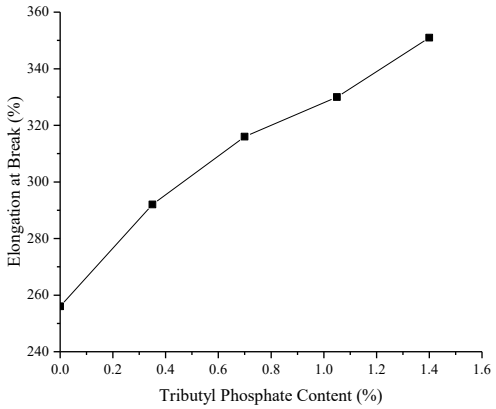

Fig. 19. Test results of elongation at break

As shown Fig. 20, the bulging and seepage water pressures increased sharply at first and then decreased slowly with the increase in defoamer content. When the defoamer content was increased, the microscopic pores of the coating gradually decreased, and the water pressure that can be borne increased accordingly. The effect of defoaming agent on increasing plasticity reduced the strength of waterproof coating, which decreased the bulging and seepage water pressures. When the content of tributyl phosphate was more than 0.7%, the bulging water pressure became equal to the seepage water pressure. This result can be ascribed to the low surface energy of tributyl phosphate, which reduced the surface tension of the coating, made the immersion liquid of waterproof coating form a deep three-dimensional network structure in the mortar block, and enhanced the adhesion between the coating and mortar. Tributyl phosphate not only increased the plasticity of the coating but also improved the adhesion between them. When the defoamer content was less than 0.7%, the difference between the bulging and seepage water pressures was large. Because of the weak bonding ability between the two groups of waterproof coatings and mortar blocks, the coating and mortar were separated during pressurization. Then, a hollow space was formed, and it can store a certain amount of seepage water until the coating was destroyed. Therefore, the difference between the bulging and seepage water pressures was large.

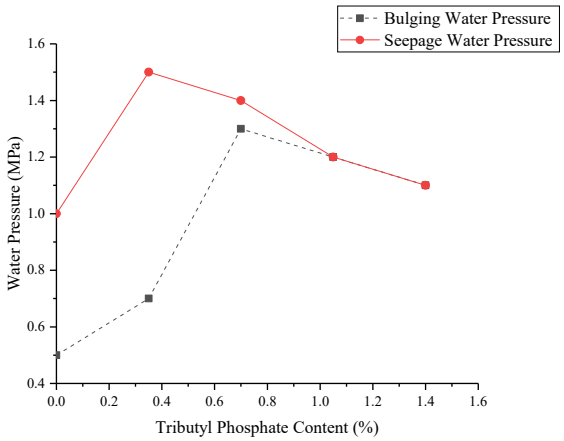

Fig. 20. Water seepage test results

From the perspective of practical engineering application, when the difference between the bulging and seepage water pressures is large, the waterproof coating in underground engineering has an early warning function. In the present study, the two-component waterborne acrylate waterproof coating had a bulging water pressure of 0.7 MPa and a seepage water pressure of 1.5 MPa when the defoamer content was 0.35%. A long warning time can be reserved before the underground project encounters a seepage accident to avoid accidents.

5. Conclusions

This study aimed to improve the performance of acrylic waterproof coating, reduce the production cost, and reveal the impermeability of waterproof coating in underground engineering. Styrene–acrylic emulsion and pure acrylic emulsion were used to prepare a waterproof coating. The effects of the ratio of two-component acrylic waterproof coating and the number of heavy calcium on the waterproofing and impermeability of the waterproof coating in underground engineering were analyzed using orthogonal and single-factor tests. The following conclusions can be drawn:

(1) When the ratio of pure acrylic emulsion and styrene–acrylic emulsion without hydrophobic modification was 0.37, the prepared waterproof coating was not permeable under the water pressure of 0.3 MPa. The physical and mechanical properties were stable, and the production cost was significantly reduced.

(2) When the ratio of pure acrylic emulsion to styrene–acrylic emulsion in the liquid component was 0.37, the proportions of alcohol ester 12, sodium hexametaphosphate solution (5% by mass), wetting agent, silane coupling agent, and tributyl phosphate were 2.5%, 3.75%, 0.2%, 0.3%, and 0.7% respectively. When the mass ratio of heavy calcium carbonate to 1250-mesh talcum powder in the solid component was 9: 1 and the liquid-powder ratio was 1: 0.93, the mechanical properties of the coating were positively correlated with the mesh number of heavy calcium carbonate. When 800-mesh heavy calcium carbonate was used, the elongation at break and tensile strength reached the maximum values of 316% and 1.11 MPa, respectively. The impermeability of 200-mesh, 325-mesh, and 600-mesh heavy calcium carbonate showed no obvious change. When 800-mesh heavy calcium carbonate was used, the bulging and seepage water pressures increased sharply to 1.3 and 1.4 MPa, respectively.

(3) As the ratio of pure acrylic emulsion to styrene–acrylic emulsion was 0.37 in the liquid phase, the proportions of alcohol ester 12, sodium hexametaphosphate solution (5% by mass), wetting agent, and silane coupling agent were 2.5%, 3.75%, 0.2%, and 0.3%, respectively. When the mass ratio of 800-mesh heavy calcium to 1250-mesh talcum powder was 9: 1 and the liquid-powder ratio was 1: 0.93, tributyl phosphate showed excellent defoaming effect on the two-component acrylic emulsion waterproof coating, which improved the compactness of the waterproof coating after drying. As the content of tributyl phosphate was increased, the elongation at break of the waterproof coating showed a positive correlation and reached the maximum value of 351%. Its tensile strength decreased slightly, and its impermeability increased sharply at first and then decreased gradually.

(4) In the impermeability test, the characteristics of the two-component acrylic emulsion waterproof coating were as follows: under the action of water pressure, the surface of the waterproof coating bulged, and the pressure continued to swell and break the coating. When the ratio of pure acrylic emulsion to styrene–acrylic emulsion in the liquid phase was 0.37, the proportions of alcohol ester 12, sodium hexametaphosphate solution (5% by mass), wetting agent, and silane coupling agent were 2.5%, 3.75%, 0.2%, and 0.3%, respectively. When the mass ratio of 800-mesh heavy calcium to 1250-mesh talcum powder was 9: 1 and the ratio of liquid to powder was 1: 0.93, the bulging water pressure reached the maximum value of 1.3 MPa when the amount of tributyl phosphate was 0.7%. The seepage water pressure reached the maximum value of 1.5 MPa when the content of tributyl phosphate was 0.35%. The coating and mortar showed different coupling relationships for different proportions in the impermeability test. When the tributyl phosphate dosage was 1.05% and 1.4%, the difference between the seepage and bulging water pressures was the smallest, which was 0 MPa. When the amount of tributyl phosphate was 0.35%, the difference was 0.8 MPa. When the difference between the bulging and seepage water

pressures was large, the waterproof coating in underground engineering can serve an early warning function to avoid underground engineering seepage accidents.

This study combined laboratory test and theoretical study and proposed an impermeability test of styrene–acrylic emulsion, pure acrylic emulsion, and waterproof coating plastering mortar. The impermeability test of the waterproof coating was simple and close to the actual situation on site. Thus, this study may serve as a reference for further studies and the development of waterproof coatings in underground engineering. Given the lack of practical application data in the project site, future studies can test the developed two-component acrylic emulsion waterproof coating in the underground engineering industry and optimize the construction technology to improve the comprehensive performance of the waterproof coating.

This is an Open Access article distributed under the terms of the Creative Commons Attribution License.

References

1. Lin, R., Liu, C. H., Lin, Z. W., Jia, Y. F., Wang, F., "Research progress of modification and functional application of water-borne acrylic coating". *Surface Technology*, 46(1), 2017, pp.133-140.
2. Shen, J., Liang, J., Lin, X., Lin, H., Yu, J., Yang, Z., "Recent progress in polymer-based building materials". *International Journal of Polymer Science*, (6), 2020, pp.1-15.
3. He, X. Y., Qin, J. Y., "*Waterproof Coating*". Beijing: Chemical Industry Press, China, 2012, pp.18-20.
4. Abd-Elnaiem, A. M., Salman, O. S., Hakamy, A., Hussein, S. I., "Mechanical characteristics and thermal stability of hybrid epoxy and acrylic polymer coating/nanoclay of various thicknesses". *Journal of Inorganic and Organometallic Polymers and Materials*, (32), 2022, pp.2094-2102.
5. Ahmed, M., Mohamed, M. K., Youcef, K., "The effect of industrial coating type acrylic and epoxy resins on the durability of concrete subjected to accelerated carbonation". *Journal of Adhesion Science and Technology*, 29(22), 2015, pp.2446-2460.
6. Vengala, J., Dharek, M. S., Sachin, D., Ghanashyam, T. B., "Thermal analysis of building model with acrylic and aluminium based roof coating materials". *Materials Today:Proceedings*, 47, 2021, pp. 3787-3793.
7. Bożena, K., Kinga, P., Piotr, K., "Polyurethane cationomer films as ecological membranes for building industry". *Progress in Organic Coatings* , 130, 2019, pp.83-92.
8. Pilch-Pitera, B., Michał, K., Olejnik, E., Zapotoczny, S., "Structure and properties of polyurethane-based powder clear coatings systems modified with hydrotalcites". *Progress in Organic Coatings*, 95, 2016, pp.120-126.
9. Jaafar, H. I., Hussein, S. I., Abd-Elnaiem, A. M., Asafa, T. B., "Effect of incorporation of conductive fillers on mechanical properties and thermal conductivity of epoxy resin composite". *Applied Physics A*, 124 (7), 2018, pp.1-7.
10. Hussein, S. I., Abd-Elnaiem, A., Ali, N., Mebed, A., "Enhanced thermo-mechanical properties of poly (vinyl alcohol)/poly (vinyl pyrrolidone) polymer blended with nanographene". *Current Nanoscience*, 16(06), 2020, pp.994-1001.
11. Jin, H. J., Young, C. H., Jeong, H. Y., Kwak, S. D., Jeong, H. M., "Waterborne polyurethane modified with poly (ethylene glycol) macromer for waterproof breathable coating". *Progress in Organic Coatings,* 103, 2016, pp.69-75.
12. Ye, X. M., Zhou, C., "Preparation and properties of one-component acrylate waterproof coatings". *China Coatings,* 33(04), 2018, pp.56-59.
13. Wu, X. H., Fu, Q. T., Kumar, D., Kanhere, P., Kanhere, P., Zhou, H., Chen, Z., "Mechanically robust superhydrophobic and superoleophobic coatings derived by sol–gel method". *Materials & Design*, 89(10), 2016, pp.1302-1309.
14. Wu, X. H., Silberschmidt, V. V., Hu, Z. T., Chen, Z., "When superhydrophobic coatings are icephobic:Role of surface topology". *Surface and Coatings Technology*, 358 (11), 2019, pp.207-214.
15. Jia, J. J., "Study on performances of different types of polymer in waterproofing coatings". *New Building Materials*, 46(05), 2019, pp. 116-119.
16. Peruchi, ABR., Zuchinali, FF., Bernardin, AM., "Development of a water-based acrylic paint with resistance to efflorescence and test method to determine the appearance of stains". *Journal of Building Engineering*, 35, 2021, pp.102005.
17. Guo, E. X., Tang, B., Wang, S. H., "A cocktail strategy for enhancing flame retardance and water resistance of butyl acrylate coatings". *Materials Chemistry and Physics*, 263, 2021, pp.124367.
18. Xiao, X., Yang, J. N., Zhang, W. D., Jiang, L. H., Qu. J., Xu, L. J., Zhang, H. Q., Song, J. R., Zhang, R. Q., Li, Y. W., Qin. J., Zhang, Z. Y., "The study of an energy efficient cool white roof coating based on styrene acrylate copolymer and cement for waterproofing purpose—Part I:Optical properties, estimated cooling effect and relevant properties after dirt and accelerated exposures". *Construction and Building Materials*, 98, 2015, pp.176-184.
19. Xiao, X., Yang, J. N., Zhang, W. D., Jiang, L. H., Qu, J., Xu, L. J., Zhang, H. Q., Song, J. R., Zhang, R. Q., Li, Y. W., Qin, J.,Zhang, Z. Y., "The study of an energy efficient cool white roof coating based on styrene acrylate copolymer and cement for waterproofing purpose—Part II:Mechanical and water impermeability properties". *Construction and Building Materials*, 96, 2015, pp.666-672.
20. Zhang, X. Y., "Study on influences of filler on tensile property of polymer emulsion architectural waterproofing coating". *China Building Waterproofing*, 34(12), 2018, pp.1-4.
21. Hu, H. B., Han, M. H., Zhang, L. L., "Hydrophobic modification of loess and its influence on the performance of waterproof coating". *Applied Chemical Industry*, 50(08), 2021, pp.2152-2156.
22. Zong, Z., Zhao, D., Dong, Y. M., Yuan, Y., Jiang, L., "Study of self-healing waterproof PU coating". *New Chemical Materials*, 49(03), 2021, pp.212-215.
23. Liu, Y. X., Lv, Y. H., Zhang, S., Wei, S. C., "Performance comparison of a few emulsions". In: *Proceedings of 2011 National Youth Conference on Tribology and Surface Engineering*, Beijing, China:Chinese Tribology Institution, 2011, pp.497-501.